e-ISSN: 2582-5208
International Research Journal of Modernization in Engineering Technology and Science
(Peer-Reviewed, Open Access, Fully Refereed International Journal)
Volume:06/Issue:01/January-2024 Impact Factor- 7.868 www.irjmets.com

CREATING INNOVATIVE PH-RESPONSIVE PMLA NANOPARTICLES FOR THE TARGETED TRANSPORT OF AMOXICILLIN TO COMBAT PATHOGENIC MICROORGANISMS

Shreya Amber*1, Kishore Kunal*2, Khushboo Kumari*3, Kumari Jyoti Sinha*4, Rupak Roy*5

*1,2,3,4Department Of Biotechnology, Patliputra University, Bihar, India.

*5SHRM Biotechnologies Pvt. Ltd., Madhyamgram, India.

Corresponding Author: Dr. Rupak Roy

DOI : https://www.doi.org/10.56726/IRJMETS47963

ABSTRACT

Thiolated chitosan/PMLA nanoparticles, featuring cysteine conjugation, were synthesized to serve as a sophisticated nano-level drug transportation system aimed at eradicating Helicobacter pylori. This bacterium notably expresses a membrane protein for importing urea in the cytoplasm and aids in supplying ammonia for its protection within the acidic stomach environment. In this research endeavor, a novel cysteine-amalgamated derivative of chitosan, termed Cys-CS, was designed and synthesized. This derivative was specifically tailored to possess mucoadhesive and anticoagulant properties, thereby facilitating its incorporation into multifunctional nanoparticles. The optimized technique allowed for the preparation of nanoparticles with the primary goal of encapsulating amoxicillin. The experimental findings revealed that antibiotic-loaded nanoparticles exhibited favorable pH-susceptible characteristics, effectively delaying the release of amoxicillin within the gastric acid milieu. This property enabled the precise delivery and targeting of the drug to Helicobacter pylori within its survival niche. Comparatively, when contrasted with unmodified antibiotic-nanoparticles conjugate, the antibiotic-loaded nanoparticles exhibited remarkable inhibition of Helicobacter pylori growth. The findings emphasize the significant promise of nanoparticles loaded with antibiotics for the efficient management of H. pylori infections.

Keywords: H Pyroli, Nanocomposites, Amoxicillin, Thiolated Chitosan, Biomaterials.

I. INTRODUCTION

The 21st Century has been marked by various environmental turmoil and threats [1, 2, 3]. Among those, antibiotic resistance is considered a serious threat [4, 5, 6]. H. pylori known for its colonization of the human gastric mucosa, has been extensively involved as a significant etiological factor of peptic ulcer disease and gastric carcinoma. This microorganism secretes urease, an enzymatic substance capable of hydrolyzing urea into ammonia and bicarbonate, serving the specific purpose of neutralizing the highly acidic pH within the gastric milieu. Consequently, the naturally low pH range (1–3) in the stomach can be raised (4-7.5) [7].

The management of H. pylori infection represents a multifaceted challenge. Multiple therapy, a combination of dual antibiotics (metronidazole, clarithromycin, or amoxicillin) along with a proton pump inhibitor (PPI), has been frequently explored. While antibacterial therapy plays a pivotal role in H. pylori eradication, the clinical utility of this approach is constrained by several inherent limitations. The rapid and extensive degradation of antimicrobial agents within the harsh acidic environment of the stomach (pH 1.2) results in inadequate drug concentrations within the gastric mucosa (pH 5.5 - 6) [8, 9, 10].

Chitosan is a naturally occurring cationic polymer derived from the N-deacetylation of chitin (2-acetamido-2-deoxy-β-D-glucan). Current investigations unveiled capacity of chitosan along its derivatives to augment the firmness of therapeutic vehicles against degradation in the gastric acid milieu, primarily attributed to their prolonged residence time within the gastrointestinal tract. Thiomer-loaded nanoparticles, part of mucoadhesive drug delivery systems, possess reactive thiol groups that enable prolonged adhesion to the mucus layer through covalent bonding with mucin glycoproteins. This interaction establishes steep drug concentration gradients, enhancing permeation at absorption sites [11, 12].

e-ISSN: 2582-5208
International Research Journal of Modernization in Engineering Technology and Science
(Peer-Reviewed, Open Access, Fully Refereed International Journal)
Volume:06/Issue:01/January-2024 Impact Factor- 7.868 www.irjmets.com

Extensively studied for their antibacterial properties, synthetic polymers, and host defense peptides feature cationic and amphiphilic structures. They aim to disrupt bacterial membranes via electrostatic interactions, integrated into the lipid domain, minimizing the risk of bacterial resistance. Peptides face challenges related to scale-up, susceptibility to enzymatic degradation, and poorly defined pharmacokinetics. Synthetic polymers encounter issues regarding biocompatibility and biodegradability. These issues may be resolved by developing amphiphilic polymers, like poly (malic acid) (PMLA). PMLA exhibits distinctive attributes, including water solubility, biodegradability, biocompatibility, non-toxicity, non-immunogenicity, and a renewable raw material source. The use of process optimization also plays a critical aspect in this regard [13, 14, 15, 16, 17, 18].

In addressing challenges posed by H. pylori infection, the investigation employed thiolated chitosan (Cys-CS) and (PMLA) to fabricate pH-responsive nanoparticles, strategically designed with mucoadhesive and anticoagulant features. This innovative method includes the encapsulation of low molecular weight antibiotics, facilitating targeted adhesion to the gastric mucosa and penetration into the mucus layer at sites of H. pylori infection. The hypothesis underlying this formulation revolves around several pivotal functions, including the safeguarding of the drug against gastric acid-induced degradation, promotion of adherence to the gastric mucosa, extension of stomach residence time, and facilitation of mucous layer penetration. Upon reaching the site of infection, these nanoparticles exhibit pH sensitivity, undergoing disintegration and thereby releasing the drug locally to target H. pylori at an elevated bacterial concentration [19, 20, 21].

In pursuit of an enhanced and highly targeted system for H. pylori eradication, this research endeavors to synthesize a cysteine-coupled chitosan derivative (Cys-CS) via amide bond formation. The successful synthesis of Cys-CS was confirmed through comprehensive characterization by ^{1}H-NMR and FTIR spectroscopy. Their properties were elucidated through a battery of analytical techniques, FT-IR spectroscopy, DLS, and TEM. The study also examined amoxicillin release from nanoparticles, tested inhibitory effects on H. pylori, and assessed the efficacy on AGS cells [22].

II. MATERIAL AND METHODS

2.1 Materials:

All the chemicals and reagents used in this study were of analytical grades and procured from Nice Chemicals Pvt. Ltd. (Kerala, India). All the microorganisms used in this study were obtained from ATCC.

2.2 Fabrication of Cys-CS conjugates:

Chitosan (CS) was modified with cysteine (Cys) through amide bond formation using EDAC/NHS. A solution containing 200 mg CS, and 400 mg Cys, and adjusted to pH 5.0 underwent a 5-hour reaction, followed by dialysis with HCl (pH 5.0±0.1) for 120 hours. [23].

2.3 Preparation of nanoparticles:

Cys-CS/PMLA and chitosan/PMLA nanoparticles were synthesized through ionic gelation at room temperature with continuous magnetic stirring. Cys-CS solutions (0.6 - 3.0 mg/mL) were prepared in 1% acetic acid adjusted to pH 4.5. PMLA solutions (0.33 - 1.67 mg/mL) were combined with Cys-CS using a flush mixing technique, creating nanoparticles at varied weight ratios (2:1 - 6:1). The resulting solutions were standardized to pH 5.5 and stirred for half an hour. DLS assessed particle size, while zeta potential was measured with a Malvern Zetasizer. Variations in pH (1.2, 6.0, and 7.0) were tested. Nanoparticle morphology was confirmed via Transmission Electron Microscopy in the Netherlands, utilizing a stained suspension on copper grids observed under transmission electron microscopy after drying for 10 minutes [24, 25].

2.4 Mucoadhesion studies with mucin:

For the mucoadhesive study equal volumes of mucin solution (0.4 mg/mL), Chitosan/PMLA Nps, and Cys-CS/PMLA Nps were vortexed for 1 min and the zeta potential of the mixtures was measured by the Malvern zetasizer USA.

2.5 Release profiles of amoxicillin-loaded nanoparticles:

Antibiotic-loaded nanoparticles, including amoxicillin-chitosan/PMLA Nps and amoxicillin-Cys-CS/PMLA Nps, were synthesized by combining amoxicillin (3 mg/mL) with PMLA (1 mg/mL, pH 7.4) and chitosan or Cys-CS solution in 1% acetic acid (1.8 mg/mL, pH 4.5). The mixture was stirred at room temperature for 30 minutes. Amoxicillin loading efficiency was quantified by centrifuging the solution at 30,000 r.p.m. for 45 minutes at 4.5

e-ISSN: 2582-5208
International Research Journal of Modernization in Engineering Technology and Science
(Peer-Reviewed, Open Access, Fully Refereed International Journal)
Volume:06/Issue:01/January-2024 Impact Factor- 7.868 www.irjmets.com

°C, and UV-Vis spectroscopy determined free amoxicillin concentration at 272 nm. Release profiles in simulated gastric media (pH 1.2, 6.0, and 7.0) at 37 °C were examined, withdrawing 4 mL at intervals and replenishing with fresh medium. Cumulative amoxicillin release was calculated based on a standard curve [26, 27].

2.6 In vitro growth inhibition study of amoxicillin-loaded nanoparticles against H. pylori

The H. pylori bacterial strain sourced from the ATCC was cultivated on blood agar plates in microaerophilic conditions at 37 °C for 2-3 days. Colonies were harvested, and combined in Hank's Balanced Salt Solution (HBSS, pH 6.0), achieving an OD590 of 1.0 (10^6 CFU/mL) via UV-Vis spectroscopy. To assess amoxicillin-loaded nanoparticles' impact on H. pylori growth, a bacterial suspension faced nanoparticles (0.5 µg/mL amoxicillin) for 6, 12, and 24 hours. OD590 measured growth inhibition, quantifying antibacterial activity compared to HBSS-treated H. pylori, following the method in the provided literature [28].

2.7 In vitro cytotoxicity of amoxicillin-loaded nanoparticles:

Cytotoxicity evaluations of amoxicillin-chitosan/PMLA or amoxicillin-Cys-CS/PMLA nanoparticles were conducted using the MTT assay with AGS cells obtained from ATCC. Cells cultured in DMEM with 10% FBS, penicillin, and streptomycin were maintained at 37 °C with 5% CO2. After detachment, cells were subcultured and used for cytotoxicity assessments. The MTT assay, relying on mitochondrial dehydrogenase activity, involved seeding 1 × 10^5 cells/mL in 96-well plates. Amoxicillin-loaded nanoparticles (0.2-1.0 mg/mL) were added, and after 24 hours, MTT solution was applied, followed by DMSO for solubilization. Absorbance was measured at 490 nm using a microplate reader with quintuplicate samples for each test and control [23].

2.8 Statistical Analysis:

Assays were performed at least thrice on separate occasions. Results show mean ± standard deviation. Significance at $p < 0.01$.

III. RESULTS AND DISCUSSION

3.1 Cysteine conjugated chitosan Synthesis:

In nanoparticle synthesis, electrostatic interactions between chitosan's C-2 amino groups and PMLA's carboxyl groups play a crucial role. To explore the effects of reducing free amino groups on nanoparticle properties and drug release, and improve chitosan permeability, we investigated incorporating cysteine (Cys) at the C-2 amino position via amide bonding, yielding Cys-CS. [29].

Cys-CS conjugates were synthesized by chemically modifying chitosan with cysteine (Cys) through amide bond formation between chitosan's free primary amino groups (CS) and cysteine's carboxyl groups. EDAC/NHS coupling agents facilitated the reaction. Cysteine's carboxyl group, pre-activated using EDAC and NHS, reacted with chitosan, yielding the desired product. After lyophilization, the resulting Cys-CS conjugate appeared as a white to pale yellow, odorless powder with a fibrous structure and demonstrated solubility across a broad pH range from 2.0 [23].

Additionally, the 1H NMR spectra confirmed the conjugation, with chitosan (CS) proton assignments: δ1.91 = CH3 (acetyl group), δ2.88 = CH (carbon 2), δ3.5–3.8 = CH + CH2 (carbons 3–6), and δ4.6 = CH (carbon 1). Notably, Cys-CS showed a distinct peak at δ3.04, indicating methylene linkages. The appearance of this peak at δ3.04, absent in chitosan, indicated successful thiol group linkage, providing conclusive evidence of amide linkages in Cys-CS (Figure 2) [30].

e-ISSN: 2582-5208
International Research Journal of Modernization in Engineering Technology and Science
(Peer-Reviewed, Open Access, Fully Refereed International Journal)
Volume:06/Issue:01/January-2024 Impact Factor- 7.868 www.irjmets.com

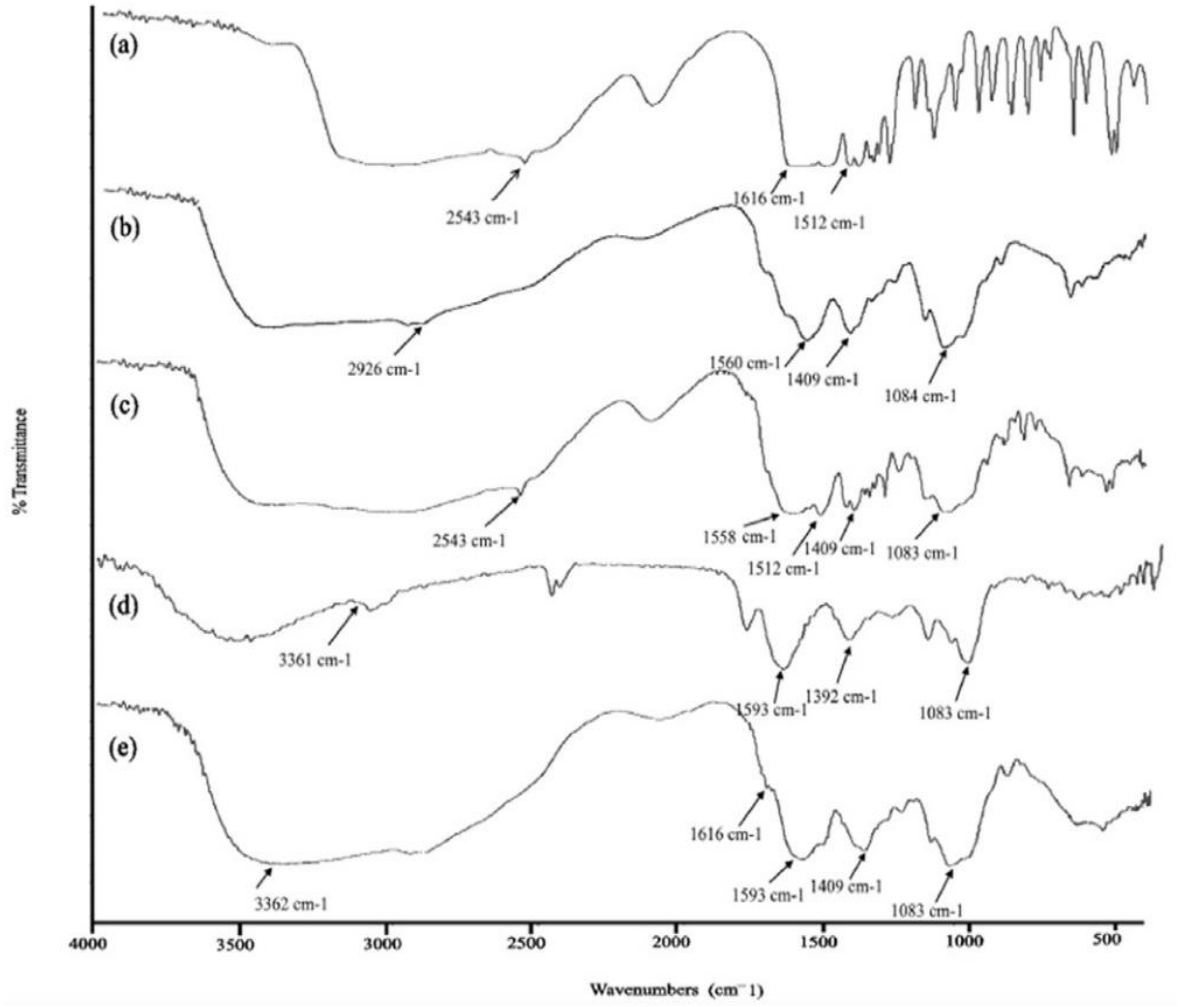

Figure 1. FT-IR spectra were obtained for (a) cysteine, (b) chitosan, (c) conjugates of cysteine and chitosan (Cys-CS), (d) poly(malic acid) (PMLA), and (e) nanoparticles composed of cysteine-chitosan conjugates and poly(malic acid) (Cys-CS/PMLA).

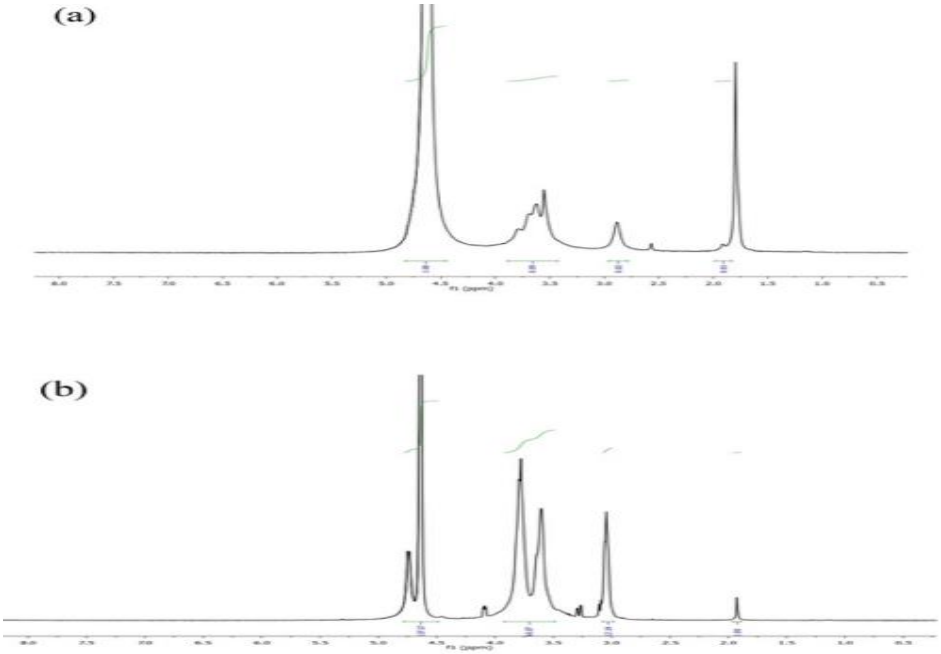

Figure 2. 1HNMR spectra of (a) chitosan and (b) cysteine conjugated chitosan Cys-CS.

e-ISSN: 2582-5208
International Research Journal of Modernization in Engineering Technology and Science
(Peer-Reviewed, Open Access, Fully Refereed International Journal)
Volume:06/Issue:01/January-2024 Impact Factor- 7.868 www.irjmets.com

3.2 Chitosan Nanoparticles: Preparation and Characterization:

Chitosan/PMLA and Cys-CS/PMLA nanoparticles were created using the ionic gelation method, leveraging electrostatic interaction between positively charged Cys-CS and negatively charged PMLA. Figures 3A and 3B depict the impact of various Cys-CS/PMLA weight ratios on particle size and zeta potential [31].

The results clearly showed that the smallest particle size occurred with a Cys-CS/PMLA weight ratio of 3:1, as shown in Figure 3A. Interestingly, as the ratio increased, Cys-CS/PMLA nanoparticles significantly increased in size compared to chitosan/PMLA nanoparticles. This is attributed to the excess Cys-CS leading to hydrophobic segment aggregation, resulting in larger particles [32].

The findings indicated the smallest particle size at a 3:1 Cys-CS/PMLA weight ratio, seen in Figure 3A. As the ratio increased, Cys-CS/PMLA particles grew larger than chitosan/PMLA.

Moreover, the concentration of the chitosan derivative, Cys-CS, significantly influenced particle size and zeta potential. Increasing Cys-CS from 0.6 to 3.0 mg/mL resulted in a noteworthy size increase at the 3:1 Cys-CS/PMLA ratio, as shown in Figure 3C. Interestingly, the size of Cys-CS/PMLA nanoparticles substantially rose at 3.0 mg/mL due to the partial conjugation of the C2 free amine group of chitosan with cysteine. This reduced the positive charge of chitosan, diminishing electrostatic interactions between Cys-CS and PMLA. In contrast, the zeta potential was minimally affected by Cys-CS concentration, maintaining a positive range of 21.47 to 29.76 mV, facilitating adhesion to negatively charged bacterial surfaces (Figure 3D). [23].

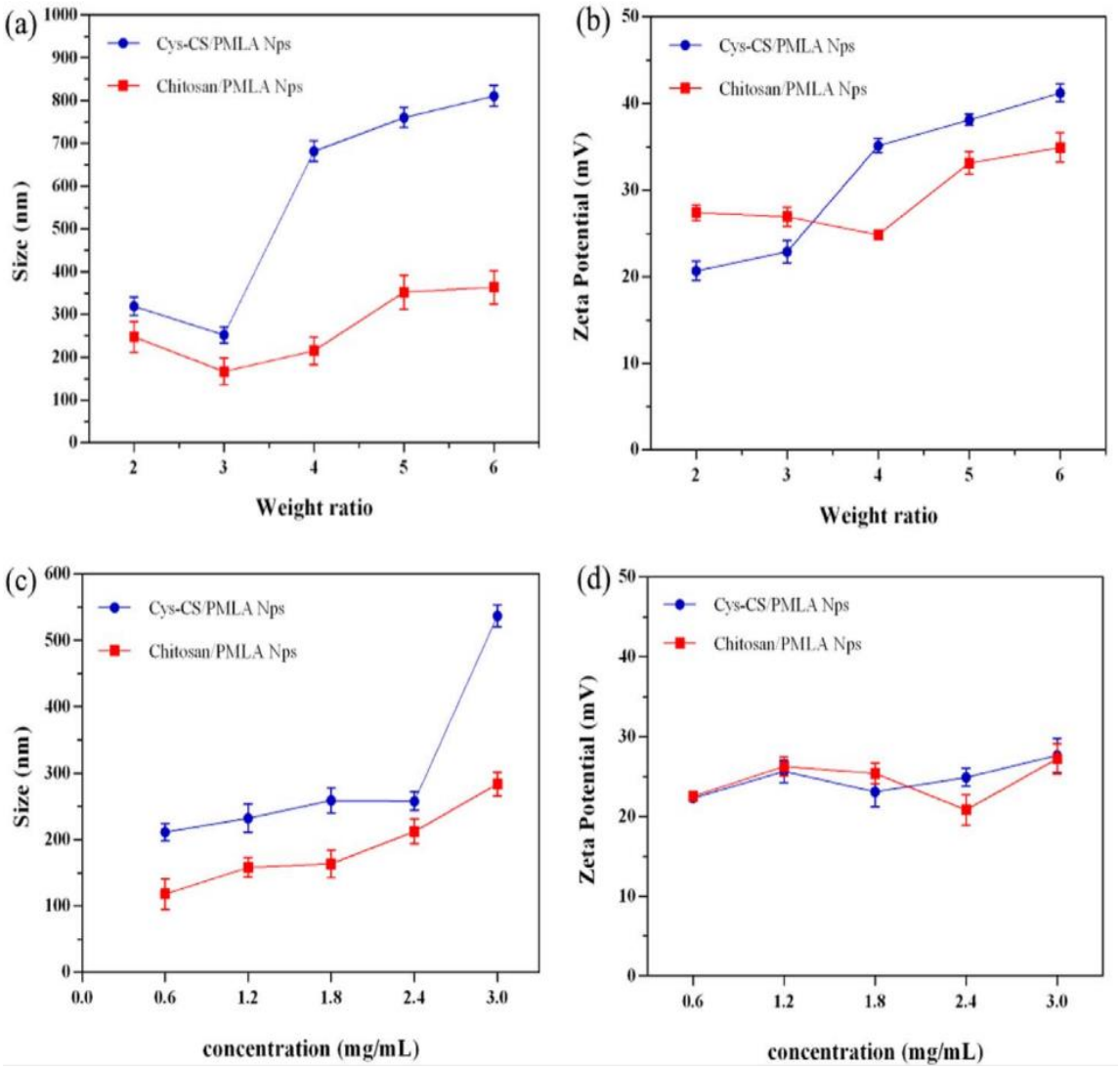

Figure 3: Influence of Cys-CS/PMLA weight ratio and Cys-CS concentration on particle size (a, c) and surface charge (b, d) at pH 5.5, determined using dynamic light scattering.

e-ISSN: 2582-5208
International Research Journal of Modernization in Engineering Technology and Science
(Peer-Reviewed, Open Access, Fully Refereed International Journal)
Volume:06/Issue:01/January-2024 Impact Factor- 7.868 www.irjmets.com

Building upon the mentioned results, the optimal conditions for preparing Cys-CS/PMLA nanoparticles were chosen as a 3:1 weight ratio and a 1.8 mg/mL Cys-CS concentration. Additionally, it's crucial to note that pH significantly affects drug release kinetics and nanoparticle stability in the gastric environment. Therefore, the behavior of Cys-CS/PMLA nanoparticles was examined under different pH conditions, and corresponding particle size and zeta potential data are illustrated in Figure 4 and Table 1.

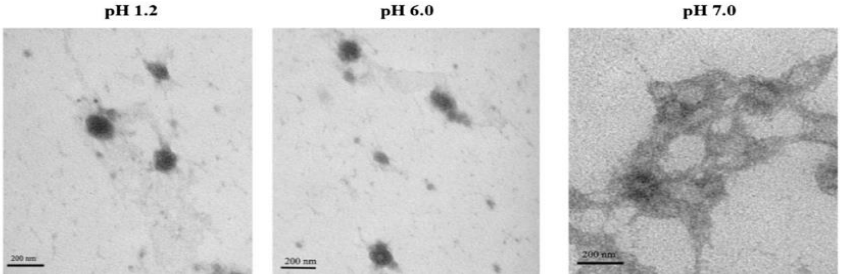

Figure 4: TEM images of the Cys-CS/PMLA nanoparticles.

Building upon the mentioned results, the optimal conditions for preparing Cys-CS/PMLA nanoparticles were chosen as a 3:1 weight ratio and a 1.8 mg/mL Cys-CS concentration. Additionally, it's crucial to note that pH significantly affects drug release kinetics and nanoparticle stability in the gastric environment. Therefore, the behavior of Cys-CS/PMLA nanoparticles was examined under different pH conditions, and corresponding particle size and zeta potential data are illustrated in Figure 4 and Table 1 [33].

Table 1: Effect of pH on various factors of Cys-CS/PMLA nanoparticles.

pH	Particle Size	PDI	Zeta Potential (mV)
1.2	188.42 ± 6.40	0.32 ± 0.02	21.16 ± 0.22
6.0	242.48 ± 17.92	0.28 ± 0.02	18.34 ± 0.20
7.0	918.28 ± 15.23	0.46 ± 0.03	17.56 ± 0.31

3.3 In vitro release profiles of amoxicillin-loaded nanoparticles:

In drug loading trials, amoxicillin-loaded Cys-CS/PMLA nanoparticles showed a size of 223.7 ± 3.2 nm and a zeta potential of 19.4 ± 0.2 mV, with 27.4 ± 3.5% loading efficiency. Compared to chitosan/PMLA nanoparticles (185.5 ± 3.6 nm, zeta potential 18.8 ± 0.3 mV, 29.7 ± 2.6% loading efficiency), amoxicillin-Cys-CS/PMLA nanoparticles closely resembled these characteristics (Table 2) [23].

Figure 5 depicts amoxicillin release profiles from nanoparticles at different pH levels over 12 hours. Both amoxicillin-chitosan/PMLA (Figure 7A) and amoxicillin-Cys-CS/PMLA nanoparticles (Figure 5B) exhibit pH-sensitive behavior. They show restrained release at pH 1.2 and more complete, sustained release at pH 6.0 and pH 7.0. The increased release at alkaline conditions is attributed to reduced electrostatic interactions between Cys-CS and PMLA. At higher pH values, weaker electrostatic associations lead to less stable nanoparticles, evidenced by larger or distorted particle sizes [34].

To replicate stomach pH variations, the release profile was studied in pH 1.2 for 2 hours, adjusted to pH 6.0 for 2 hours, and maintained at pH 7.0 for 8 hours (Figure 5C). Even with dynamic pH changes, amoxicillin maintained favorable pH-sensitive behavior, preventing premature release in gastric acid and facilitating effective drug delivery to Helicobacter pylori survival zones.

Table 2: Physicochemical characteristics of amoxicillin-Cys-CS/PMLA nanoparticles and amoxicillin-chitosan/PMLA nanoparticles

Conjugate Description	Particle Size (mm)	Zeta- Potential (mV)	L.E. (%)
Amoxicillin-Cys-CS/PMLA NanoParticles	218.47 ± 1.32	18.56 ± 0.92	27.21 ± 1.45
Amoxicillin-chitosan/ PMLA NanoParticles	178.44 ± 1.63	17.24 ± 0.18	32.14 ± 1.86

e-ISSN: 2582-5208
International Research Journal of Modernization in Engineering Technology and Science
(Peer-Reviewed, Open Access, Fully Refereed International Journal)
Volume:06/Issue:01/January-2024 Impact Factor- 7.868 www.irjmets.com

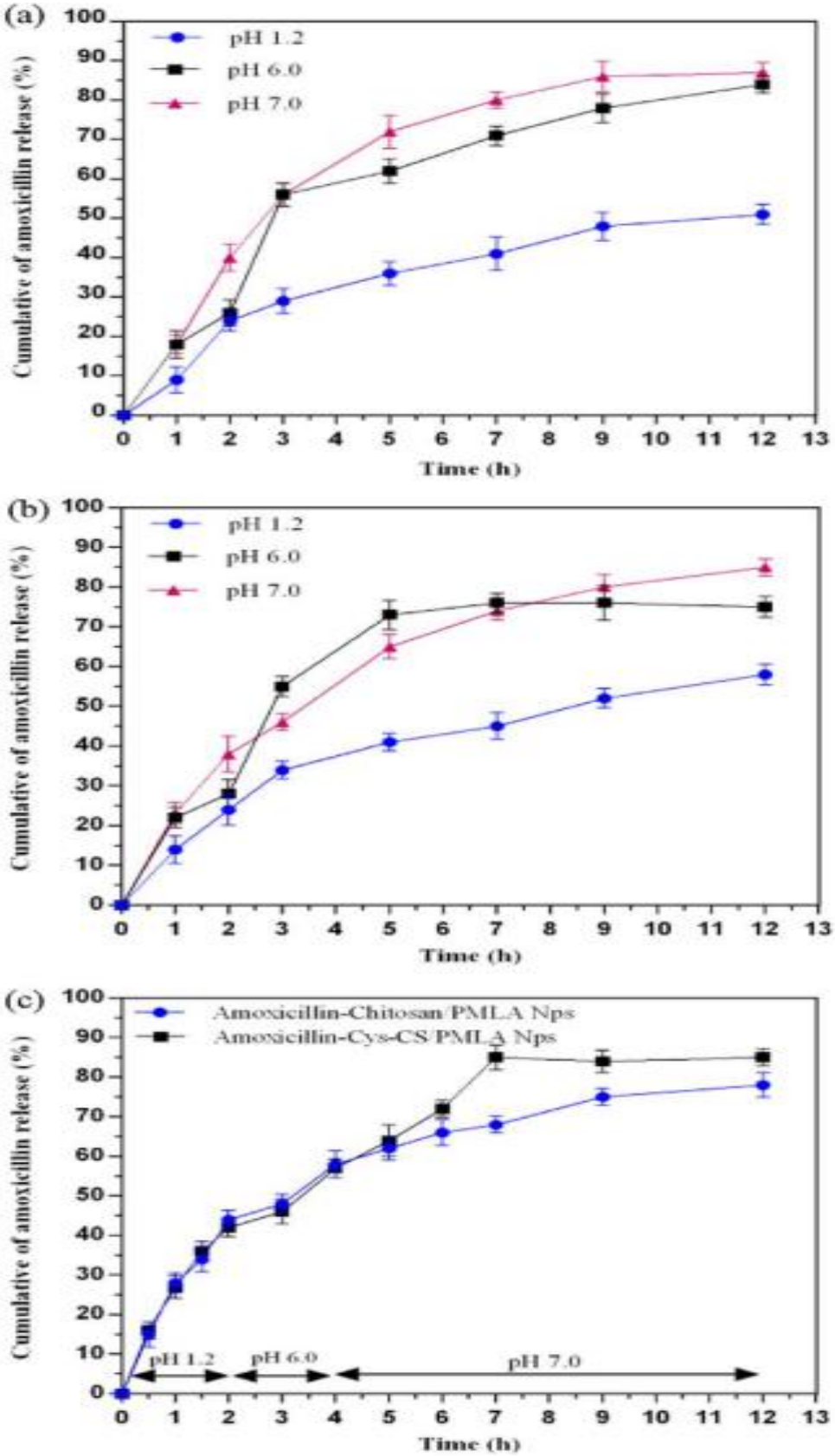

Figure 5: Amoxicillin release rates at varied pH values were studied for amoxicillin-chitosan/PMLA nanoparticles (a) and amoxicillin-Cys-CS/PMLA nanoparticles (b). Additionally, the nanoparticles underwent pH changes (c) at 37 ± 1 °C, including pH 1.2 for 2 hours, pH 6.0 for 2 hours, and pH 7.0 for 8 hours.

e-ISSN: 2582-5208
International Research Journal of Modernization in Engineering Technology and Science
(Peer-Reviewed, Open Access, Fully Refereed International Journal)
Volume:06/Issue:01/January-2024 Impact Factor- 7.868 www.irjmets.com

3.4 Growth inhibition against H. pylori:

Figure 6A illustrates the percentage of growth inhibition of H. pylori following treatment with amoxicillin-loaded nanoparticles—amoxicillin-chitosan/PMLA and amoxicillin-Cys-CS/PMLA, both at an amoxicillin concentration of 0.5 µg/mL. Blank nanoparticles (without amoxicillin) data are also presented over time intervals (6, 12, and 24 hours).

The figure reveals several key observations:

- Blank Nanoparticles: Neither type of blank nanoparticles, devoid of amoxicillin, inhibited H. pylori growth even after 24 hours, indicating no adverse impact on bacterial proliferation.
- Time-Dependent Inhibition: Growth inhibition of H. pylori increased gradually over the tested time intervals.
- Amoxicillin-Cys-CS/PMLA Superiority: Amoxicillin-Cys-CS/PMLA nanoparticles, featuring cysteine-conjugated chitosan, exhibited significantly superior growth inhibitory activity against H. pylori compared to equivalent amoxicillin-chitosan/PMLA nanoparticles.
- Direct Interaction: Amoxicillin-Cys-CS/PMLA nanoparticles, with a positive surface charge, exhibited enhanced direct interaction with H. pylori. After 6 hours, they achieved a 48.62% growth inhibition, surpassing amoxicillin-chitosan/PMLA nanoparticles. After 24 hours, the inhibition reached 77.1%, emphasizing their heightened efficacy [35].

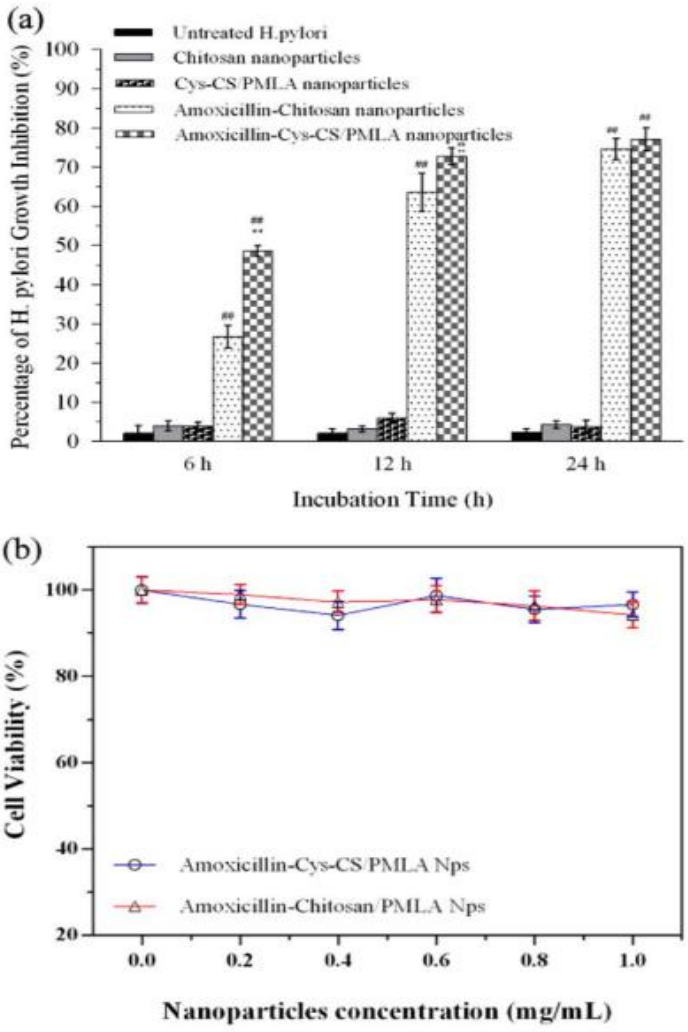

Figure 6: a) H. pylori growth inhibition percentages for various amoxicillin-loaded nanoparticles and their blank counterparts at defined time intervals (n = 3). ##p < 0.01 for blank nanoparticles vs. untreated group or amoxicillin-loaded nanoparticles vs. blank nanoparticles, **p < 0.01 compared to amoxicillin-chitosan/PMLA nanoparticles. (b) Cell viability post-treatment with amoxicillin-loaded Cys-CS/PMLA and amoxicillin-loaded CS/PMLA NPs at specific times, assessed via MTT assay.

e-ISSN: 2582-5208
International Research Journal of Modernization in Engineering Technology and Science
(Peer-Reviewed, Open Access, Fully Refereed International Journal)
Volume:06/Issue:01/January-2024 Impact Factor- 7.868 www.irjmets.com

3.5 Cytotoxicity of synthesized nanoparticles:

Using the MTT assay, cytotoxicity of different concentrations of amoxicillin-loaded Cys-CS/PMLA and chitosan/PMLA nanoparticles was evaluated. Viability remained unaffected below 0.8 mg/mL, with a slight decrease at concentrations above 1.0 mg/mL (Figure 6B).

Moreover, no statistically significant difference in overall cell survival was observed between chitosan/PMLA and Cys-CS/PMLA nanoparticles. These results collectively indicate that Cys-CS, even after chemical modification, maintains safety and lacks cytotoxicity. In summary, MTT assay results confirm the biocompatibility of both nanoparticle types at lower concentrations, highlighting the safety of cysteine-conjugated chitosan derivative, Cys-CS, for biomedical applications [23].

IV. CONCLUSION

In this investigation, we designed Cys-CS/PMLA nanoparticles using a synthetic cysteine-conjugated chitosan derivative, employing a straightforward ionic gelation method. Our results unequivocally demonstrated pH-sensitive release and drug-loading efficiency comparable to other formulations. Our mucoadhesive experiments provided strong evidence of excellent mucoadhesive properties attributed to intermolecular interactions, such as disulfide bonds, with mucin layer glycoproteins. Investigations into Helicobacter pylori growth inhibition affirmed Cys-CS/PMLA nanoparticles' ability to effectively deliver amoxicillin, facilitating targeted and efficient eradication. This development offers novel insights into pH-sensitive cysteine-conjugated nanocarriers, promising for oral drug delivery, specifically targeting Helicobacter pylori and enhancing local drug bioavailability. In conclusion, this study successfully designed Cys-CS/PMLA nanoparticles, opening avenues for innovative pH-sensitive nanocarriers to improve Helicobacter pylori treatment effectiveness.

CONFLICT OF INTEREST: No potential Conflict of Interest was reported in the reported study.

STATEMENT ON AUTHOR'S CONTRIBUTION: Shreya Amber and Kishore Kunal may be regarded as the 1st authors of this study since they have done most of the experimentation and data analysis of this work. Khushboo Kumari and Kumari Jyoti Sinha may be considered as the 2nd authors of this manuscript as they have performed the data presentation and writing of the manuscript. Dr. Rupak Roy may be considered as the corresponding author of the manuscript since he has designed, conceptualized, supervised, and revised the entire project.

V. REFERENCES

[1] Roy, R., & Ray, S. (2020). Development of a non-linear model for prediction of higher heating value from the proximate composition of lignocellulosic biomass. Energy Sources, Part A: Recovery, Utilization, and Environmental Effects, 1-14.

[2] Roy, R., & Ray, S. (2022). Upgradation of an Agro-residue by Acid Pretreatment into a Solid Fuel with Improved Energy Recovery Potential: An Optimization Study. Arabian Journal for Science and Engineering, 47(5), 6311-6323.

[3] Roy, R., & Ray, S. (2019). Effect of various pretreatments on energy recovery from waste biomass. Energy Sources, Part A: Recovery, Utilization, and Environmental Effects, 1-13.

[4] Parveen, S., Sur, T., Sarkar, S., & Roy, R. (2023). Antagonist Impact of Selenium-Based Nanoparticles Against Mycobacterium tuberculosis. Applied Biochemistry and Biotechnology, 1-9.

[5] Ghosal, A., Roy, R., Sharma, K., Mitra, P., & Vora, K. (2022). Antibiofilm activity of Phytocompounds against of Staphylococcus aureus Biofilm forming Protein-In silico study. American Journal of Applied Bio-Technology Research, 3(1), 27-29.

[6] Li, R., & Roy, R. (2023). Gut Microbiota and Its Role in Anti-aging Phenomenon: Evidence-Based Review. Applied Biochemistry and Biotechnology, 1-15.

[7] Nejati, S., Karkhah, A., Darvish, H., Validi, M., Ebrahimpour, S., & Nouri, H. R. (2018). Influence of Helicobacter pylori virulence factors CagA and VacA on pathogenesis of gastrointestinal disorders. Microbial pathogenesis, 117, 43-48.

[8] Su, Q., Dong, J., Zhang, D., Yang, L., & Roy, R. (2022). Protective effects of the bilobalide on retinal oxidative stress and inflammation in streptozotocin-induced diabetic rats. Applied Biochemistry and Biotechnology, 194(12), 6407-6422.

[9] Song, B., Liu, X., Dong, H., & Roy, R. (2023). miR-140-3P Induces Chemotherapy Resistance in Esophageal Carcinoma by Targeting the NFYA-MDR1 Axis. Applied Biochemistry and Biotechnology, 195(2), 973-991.

[10] Qiu, S., Wu, X., Wu, Q., Jin, X., Li, H., & Roy, R. (2023). Pharmacological Action of Baicalin on Gestational Diabetes Mellitus in Pregnant Animals Induced by Streptozotocin via AGE-RAGE Signaling Pathway. Applied Biochemistry and Biotechnology, 1-16.

[11] Taubner, T., Marounek, M., & Synytsya, A. (2020). Preparation and characterization of hydrophobic and hydrophilic amidated derivatives of carboxymethyl chitosan and carboxymethyl β-glucan. International Journal of Biological Macromolecules, 163, 1433-1443.

[12] Roy, R., Chakraborty, A., Jana, K., Sarkar, B., Biswas, P., & Madhu, N. R. (2023). The Broader Aspects of Treating Diabetes with the Application of Nanobiotechnology. In Advances in Diabetes Research and Management (pp. 137-162). Singapore: Springer Nature Singapore.

[13] Roy, R., Shil, S., Choudhary, D. K., Mondal, P., Adhikary, P., Manna, U., ... & Maji, M. (2022). Conversion of glucose into calcium gluconate and determining the process feasibility for further scaling-up: An optimization approach. Int. J. Exp. Res. Rev, 27, 1-10.

[14] Dey, P., Roy, R., Mukherjee, A., Krishna, P. S., Koijam, R., & Ray, S. (2022). Valorization of Waste Biomass as a Strategy to Alleviate Ecological Deficit: A Case Study on Waste Biomass Derived Stable Carbon. Advanced Microscopy, 167-196.

[15] Roy, R., Debnath, D., & Ray, S. (2022). Comprehensive assessment of various lignocellulosic biomasses for energy recovery in a hybrid energy system. Arabian Journal for Science and Engineering, 47(5), 5935-5948.

[16] Roy, A. A. B. R. Impact of different process parameters on the quality of raw milk: an optimization-based approach.

[17] Roy, R. (2022). Assessment on Energy Utilization from Various Lignocellulosic Biomass.

[18] Vipparla, C., Sarkar, S., Manasa, B., Pattela, T., Nagari, D. C., Aradhyula, T. V., & Roy, R. (2022). Enzyme Technology in Biofuel Production. In Bio-Clean Energy Technologies Volume 2 (pp. 239-257). Singapore: Springer Nature Singapore.

[19] Banik, S., Nath, P. C., & Roy, R. (2023). Microbiome and gut-brain axis affecting stress behavior. American Journal of Applied Bio-Technology Research, 3(4), 17-34.

[20] Roy, R., Srinivasan, A., Bardhan, S., & Paul, T. (2022). Evaluation of the Expression of CD-4 and CD-45 Count among Patients Having Non-Small Cell Lung Cancer. Journal homepage: www. ijrpr. com ISSN, 2582, 7421.

[21] Bashar, S., Bardhan, S., & Roy, R. (2022). An optimization-based study of the impact of different parameters on DNA degradation. Int. J. Exp. Res. Rev, 28, 1-7.

[22] Roy, R., Sarkar, S., Kotak, R., Nandi, D., Shil, S., Singha, S., ... & Tarafdar, S. (2022). Evaluation of the Water Quality Parameters from Different Point Sources: A Case Study of West Bengal. American Journal of Applied Bio-Technology Research, 3(3), 18-28.

[23] Jing, Z. W., Jia, Y. Y., Wan, N., Luo, M., Huan, M. L., Kang, T. B., ... & Zhang, B. L. (2016). Design and evaluation of novel pH-sensitive ureido-conjugated chitosan/TPP nanoparticles targeted to Helicobacter pylori. Biomaterials, 84, 276-285.

[24] Huang, X., Xu, L., Qian, H., Wang, X., & Tao, Z. (2022). Polymalic acid for translational nanomedicine. Journal of Nanobiotechnology, 20(1), 295.

[25] Austin, J., Minelli, C., Hamilton, D., Wywijas, M., & Jones, H. J. (2020). Nanoparticle number concentration measurements by multi-angle dynamic light scattering. Journal of Nanoparticle Research, 22(5), 108.

[26] Goyal, A. K., Rath, G., Faujdar, C., & Malik, B. (2019). Application and perspective of pH-responsive nano drug delivery systems. In Applications of Targeted Nano Drugs and Delivery Systems (pp. 15-33). Elsevier.

[27] Aflakian, F., Mirzavi, F., Aiyelabegan, H. T., Soleimani, A., Navashenaq, J. G., Karimi-Sani, I., ... & Vakili-Ghartavol, R. (2023). Nanoparticles-based therapeutics for the management of bacterial infections: a special emphasis on FDA approved products and clinical trials. European Journal of Pharmaceutical Sciences, 106515.

[28] Kinoshita-Daitoku, R., Ogura, Y., Kiga, K., Maruyama, F., Kondo, T., Nakagawa, I., ... & Mimuro, H. (2020). Complete genome sequence of Helicobacter pylori strain ATCC 43504, a type strain that can infect gerbils. Microbiology Resource Announcements, 9(18), 10-1128.

[29] Liu, K., Jiang, X., & Hunziker, P. (2016). Carbohydrate-based amphiphilic nano delivery systems for cancer therapy. Nanoscale, 8(36), 16091-16156.

[30] Lavertu, M., Xia, Z., Serreqi, A. N., Berrada, M., Rodrigues, A., Wang, D., ... & Gupta, A. (2003). A validated 1H NMR method for the determination of the degree of deacetylation of chitosan. Journal of pharmaceutical and biomedical analysis, 32(6), 1149-1158.

[31] Huang, X., Xu, L., Qian, H., Wang, X., & Tao, Z. (2022). Polymalic acid for translational nanomedicine. Journal of Nanobiotechnology, 20(1), 295.

[32] Safarov, T., Kiran, B., Bagirova, M., Allahverdiyev, A. M., & Abamor, E. S. (2019). An overview of nanotechnology-based treatment approaches against Helicobacter Pylori. Expert review of anti-infective therapy, 17(10), 829-840.

[33] Chang, C. H., Lin, Y. H., Yeh, C. L., Chen, Y. C., Chiou, S. F., Hsu, Y. M., ... & Wang, C. C. (2010). Nanoparticles incorporated in pH-sensitive hydrogels as amoxicillin delivery for eradication of Helicobacter pylori. Biomacromolecules, 11(1), 133-142.

[34] Reza, M. S., Quadir, M. A., & Haider, S. S. (2003). Comparative evaluation of plastic, hydrophobic and hydrophilic polymers as matrices for controlled-release drug delivery. J Pharm Pharm Sci, 6(2), 282-291.

[35] Safarov, T., Kiran, B., Bagirova, M., Allahverdiyev, A. M., & Abamor, E. S. (2019). An overview of nanotechnology-based treatment approaches against Helicobacter Pylori. Expert review of anti-infective therapy, 17(10), 829-840.